

Electrical properties and Al-doping site analysis of (002)-oriented Al-doped ZnO thin films prepared by chemical bath deposition

DONGYUN GUO^{a,*}, LONG LIU^a, XINYI LI^a, ZHIXIONG HUANG^a, LIANMENG ZHANG^a, KAZUMI KATO^b

^a*School of Materials Science and Engineering, Wuhan University of Technology, Wuhan 430070, China*

^b*National Institute of Advanced Industrial Science and Technology, Tsukuba 305-8560, Japan*

The highly (002)-oriented Al-doped ZnO (AZO) thin films were prepared by a chemical bath deposition, and the doping sites of Al³⁺ ions in ZnO thin films was investigated. All AZO films had high transparency in the visible wavelength range, while they showed poor electrical conductivity. The resistivity of these AZO thin films varied from 1.10×10^{-2} to $4.64 \times 10^{-2} \Omega \cdot \text{cm}$. As the AZO thin films were prepared by the chemical bath deposition, the substitution of Al³⁺ ions for Zn²⁺ ions was quite difficult in the ZnO crystal structure, and then the Al³⁺ ions mainly segregated at the grain boundaries, which induced the low electrical conductivity.

(Received March 23, 2019; accepted February 17, 2020)

Keywords: Al-doped ZnO thin film, Chemical bath deposition, (002) orientation, Carrier concentration, Carrier mobility

1. Introduction

Transparent conductive oxide thin films have attracted lots of attention due to their unique combination of high transparency and low resistivity, which makes them to be key components in the field of optoelectronic devices [1]. Al-doped ZnO (AZO), due to its excellent optical and electrical properties, represents a lower cost, non-toxicity and earth-abundant alternative to the well-known transparent conductive oxide thin film, indium tin oxide (ITO) [2-4]. The (002)-oriented ZnO thin films showed higher electrical conductivity compared to the random-oriented ZnO thin film due to high carrier mobility along the *c*-axis, which indicated that the (002)-oriented AZO thin films should be prepared to obtain high conductivity [5].

Chemical bath deposition can prepare films at low temperature with low cost. Chandramohan *et al*[6] prepared (002)-oriented AZO thin films on glass substrates by the chemical bath deposition with good optical properties. Verrier *et al*[7] investigated the effect of pH value on formation and doping mechanisms of ZnO nanowires prepared by the chemical bath deposition. Recently, Advand *et al*[8] reported the field emission performance of AZO nanorods prepared by the chemical bath deposition. However, in these literature, the electrical properties of AZO films were almost neglected. In this study, the AZO thin films were prepared on Si(100) and fused quartz glass substrates with (002)-oriented ZnO nucleation layer by the chemical bath deposition, and their electrical and optical properties were investigated. The doping sites of Al³⁺ ions in ZnO crystal structure was analyzed.

2. Experimental details

All the reagents were of analytical grade purity and were used without further purification. The (002)-oriented

ZnO nucleation layer were prepared on Si(100) and fused quartz glass substrates by sol-gel method [9-11]. The AZO thin films were grown on the (002)-oriented ZnO nucleation layer by the chemical bath deposition. The desired amounts of Zn(Ac)₂·2H₂O and Al(NO₃)₃·9H₂O were dissolved in deionized water to form the Al-Zn precursors, and then hexamethylenetetramine (HMT) was added to the Al-Zn precursors. In the Al-Zn precursors, the molar ratio of HMT to Zn(Ac)₂·2H₂O and Al(NO₃)₃·9H₂O was kept at 1 or 2, and the concentration of Al³⁺ and Zn²⁺ ions was 0.1 mol/L. As the Al-Zn precursors were heated at 60 or 70 °C, the substrates with the (002)-oriented ZnO nucleation layer were immersed in the precursors for different time. The as-deposited samples were post-annealed at 400 °C for 30 min in H₂ gas to increase their conductivity. The details of AZO samples prepared by the chemical bath deposition are listed in Table 1.

The crystal phase of these samples was measured by an X-ray diffractometer (XRD, RINT-2100V, Rigaku) with CuK α radiation (40 kV, 30 mA). The scanning rate was 1 °/min with a scanning step of 0.01 °. The morphologies of the AZO films were characterized using a field emission scanning electron microscope (FESEM, JSM-6335FM, JEOL) and a high-resolution transmission electron microscopy (HR-TEM, Hitachi H-9000UHR III). The elements of the AZO thin film were studied by a scanning transmission electron microscopy and energy-dispersive X-ray analysis (STEM-EDX, JEOL JEM2100F and JED-2300T). The electrical properties were characterized with a Hall measurement system (ResiTest 8300, Toyo), and the optical properties were measured using an ultraviolet-visible-near infrared spectrophotometer (UV-3100PC, Shimadzu).

Table 1. Details of AZO samples prepared by chemical bath deposition

Samples no.		1	2	3	4	5	6	7	8
Substrate		Fused quartz glass							Si(100)
ZnO nucleation layer		(002)-oriented ZnO nucleation layer							
AZO thin film	HMT/(Al+Zn)	1	1	2	1	1	1	1	2
	Concentration (mol/L)	0.1							
	Al content (at.%) [*]	3	5	10	3	3	3	5	10
	Deposition temperature and time(°C/min)	60/120	60/120	60/120	60/210	60/180	60/120	60/120	70/40
	H ₂ treatment (°C/min)	400/30							-
Total film thickness (nm)		320	320	280	550	450	300	270	310
Electrical properties	Resistivity ($\times 10^{-2} \Omega \cdot \text{cm}$)	1.67	1.10	2.50	3.08	4.64	3.31	1.50	-
	Carrier concentration ($\times 10^{19} \text{ cm}^{-3}$)	2.58	2.83	3.96	1.84	1.82	4.29	4.40	-
	Mobility ($\text{cm}^2/(\text{V} \cdot \text{s})$)	14.5	20.0	6.3	11.0	7.4	4.4	9.5	-
Optical transmittance in the visible wavelength region		More than 80%							-

^{*} The values represented the molar ratio of Al³⁺ ions to (Zn²⁺+Al³⁺) ions in the solutions

3. Results and discussion

The AZO thin films were deposited on the fused quartz glass substrates with (002)-oriented ZnO nucleation layers by the chemical bath deposition at 60 °C. The process parameters of heating time, molar ratio of HMT/(Zn²⁺+Al³⁺) and Al³⁺ content in the Al-Zn precursors were changed. The typical XRD patterns of the AZO thin films (samples No. 1, 2 and 3) are displayed in Fig. 1. All AZO thin films showed strong (002) orientation, which were indexed to JCPDS 36-1451. With increasing the Al content in the Al-Zn precursors, the intensity of (002) peak for AZO thin films obviously increased. Figure 2 shows the typical morphologies of the AZO thin films (samples No. 1, 2 and 3). As the AZO thin film was prepared with Al content of 3 at.% in the Al-Zn precursor, the AZO grains grew close contact together, and the incomplete hexagonal grains were observed. When the AZO thin film was prepared with Al content of 5 at.% in the Al-Zn precursor, the complete hexagonal grains were observed. With increasing the Al content in the Al-Zn precursor to 10 at.%, the AZO thin film consisted of the complete hexagonal grains, and the grain size obviously decreased. All AZO thin films had the columnar cross-section, and the film thicknesses of these samples were measured according to the cross-sectional SEM images. All these samples showed the similar oriented growth and morphologies, and they also had high transparency in the visible wavelength range.

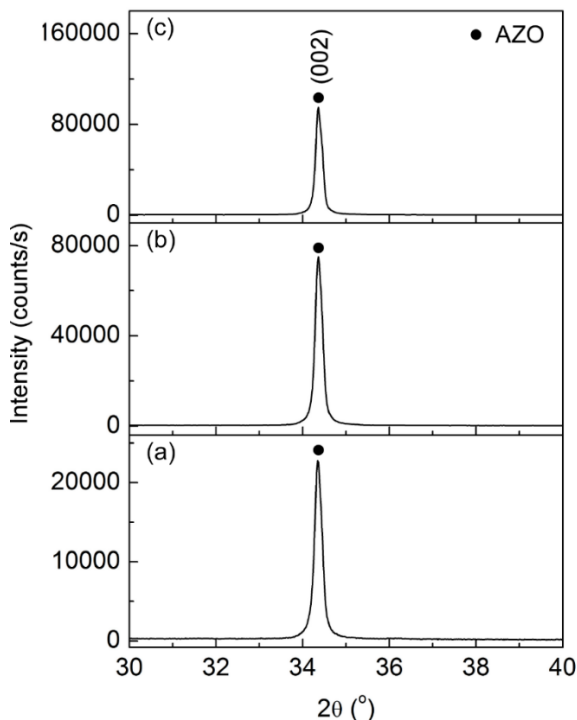


Fig. 1. The typical XRD patterns of AZO thin films (samples no. 1(a), 2(b) and 3(c)) prepared on the fused quartz glass substrate with (002)-oriented ZnO nucleation layer by chemical bath deposition with different Al contents in the Al-Zn precursors

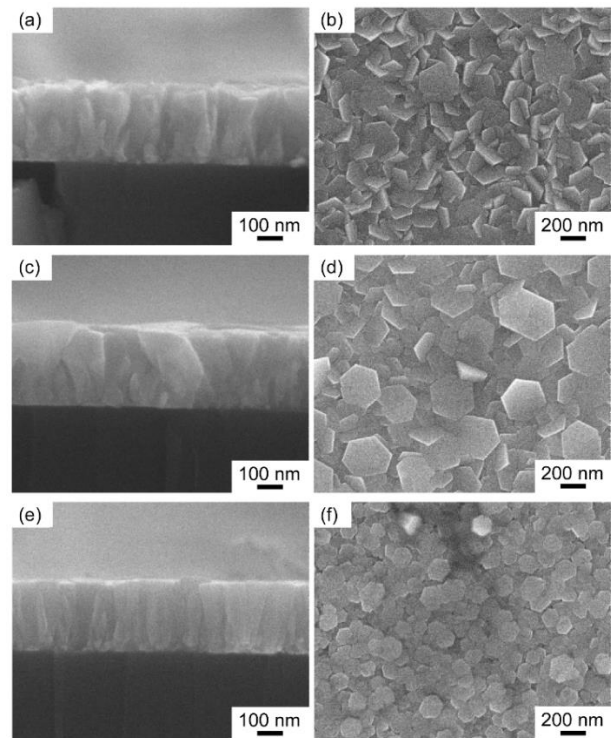


Fig. 2. The typical cross-sectional and surface morphologies of AZO thin films (samples no. 1(a, b), 2(c, d) and 3(e, f)) prepared on the fused quartz glass substrates with (002)-oriented ZnO nucleation layer by chemical bath deposition with different Al contents in the Al-Zn precursors

To achieve good electrical conductivity for transparent electrode, the carrier concentrations and mobility should be as high as possible. In this study, the resistivity (ρ) of the AZO thin films varied from $1.10 \times 10^{-2} \Omega \cdot \text{cm}$ to $4.64 \times 10^{-2} \Omega \cdot \text{cm}$, the carrier concentration ranged from $1.82 \times 10^{19} \text{ cm}^{-3}$ to $4.40 \times 10^{19} \text{ cm}^{-3}$, and the carrier mobility varied from $4.40 \text{ cm}^2/(\text{V} \cdot \text{s})$ to $20.0 \text{ cm}^2/(\text{V} \cdot \text{s})$. Birkholz *et al* [5] investigated the structure-function relationship between preferred orientation and electrical resistivity in the AZO thin films, and the high density of (002)-oriented grains exhibited a high degree of parallel alignment and thereby caused an increase of the inter-grain mobility. According to the XRD (Fig. 1) and SEM (Fig. 2) results, the AZO thin films showed strong (002) orientation with columnar cross-section, which indicated that the AZO thin films could have high carrier mobility, such as $20.0 \text{ cm}^2/(\text{V} \cdot \text{s})$. However, compared with the AZO thin films prepared by pulsed laser deposition[12], chemical vapor deposition[13], sputtering[14] and sol-gel method[9], the AZO films prepared by the chemical bath deposition had relatively low carrier concentration. As the Al content varied from 3 at.% to 10 at.% in the Al-Zn precursors, the carrier concentration of the samples almost didn't change. Aluminum ions were n-type dopants, and the Al doping could increase the free-electron concentration in the AZO films, which indicated that the Al doping played an important role in their carrier concentration. It is necessary

to investigate the Al-doping sites in the ZnO thin films prepared by the chemical bath deposition.

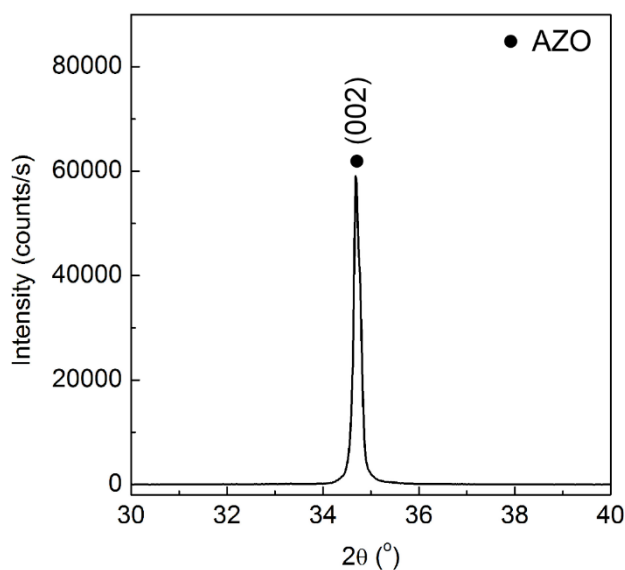


Fig. 3. XRD pattern of AZO thin film prepared on Si substrate with (002)-oriented ZnO nucleation layer by chemical bath deposition

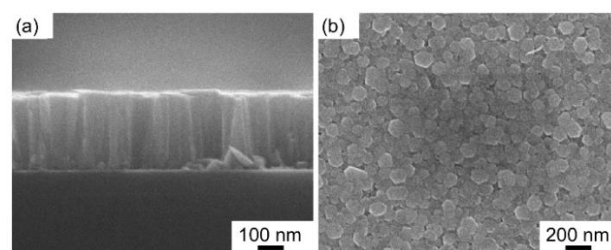


Fig. 4. Cross-sectional and surface morphologies of AZO thin film prepared on Si substrate with (002)-oriented ZnO nucleation layer by chemical bath deposition

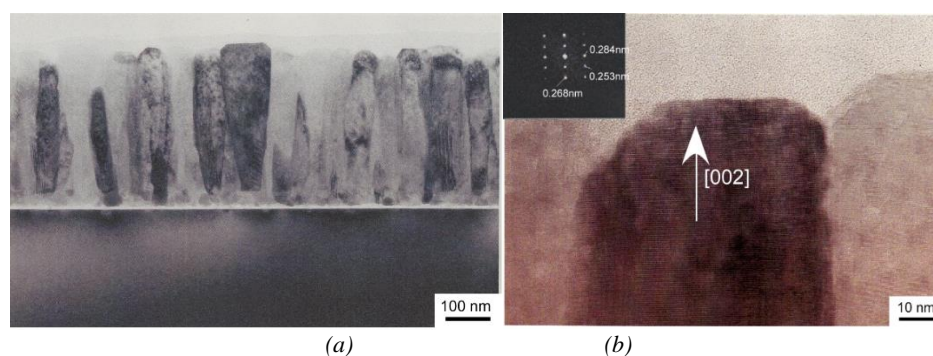


Fig. 5. (a) Cross-sectional TEM image of AZO thin film deposited on Si substrate, (b) HR-TEM image of columnar AZO grain and the inset is the fast Fourier transformation (FFT) pattern (color online)

The AZO thin film (sample No. 8) was deposited on Si substrate with (002)-oriented ZnO nucleation layer. The molar ratio of HMT to $\text{Zn}(\text{Ac})_2 \cdot 2\text{H}_2\text{O}$ and $\text{Al}(\text{NO}_3)_3 \cdot 9\text{H}_2\text{O}$ was kept at 2, and the Al content in the Al-Zn precursor was 10 at.%. The Si substrate with the (002)-oriented ZnO nucleation layer was immersed in the Al-Zn precursor at 70 °C for 40 min. Figure 3 shows the XRD result of this sample (No. 8). The highly (002)-oriented AZO thin film was obtained. The AZO film consisted of hexagonal grains with columnar cross-section as shown in Fig. 4. Fig. 5 displays the TEM images and fast Fourier transformation (FFT) pattern for cross-section of AZO thin film deposited on Si substrate. The AZO columnar grains were clearly observed as shown in Fig. 5(a). According to the HR-TEM image of Fig. 5(b), the interplanar spacings of 0.268, 0.253 and 0.284 nm corresponded to (002), (101) and (100) planes of AZO phase, respectively. This result indicated that the AZO columnar grain grew along the [002]

direction.

Fig. 6 shows the cross-sectional high-angle annular dark field (HAADF) STEM image and its EDX results of the AZO thin film deposited on Si substrate. The Al^{3+} ions distribution in the columnar AZO grains was analyzed by HAADF-STEM in combination with EDX analysis. The presence of Al element was confirmed by the EDX spectrum, as shown in Fig. 6(b). The three different regions (top, middle and bottom) of a single AZO columnar grain were analyzed. According to the EDX spectra of Figs. 6(c), (d) and (e), the Al element was not detected in the single columnar grain. Nasr *et al* [15] investigated the Al^{3+} ions distribution in the AZO thin films, the Al^{3+} ions tended to segregate at the grain boundaries or free surface. In this study, as the thin films were prepared at low temperature (60 and 70 °C) and normal pressure, the Al^{3+} ions mainly segregated at the grain boundaries, and the substitution of Al^{3+} ions for Zn^{2+} ions was quite difficult due to the

difference in oxidation state, ionic radius and coordination preference. This conclusion could explain why the existence of Al element was confirmed for the whole cross-section (Fig. 6(b)), and the effect of Al doping in the

single columnar grain was negligible (Figs. 6(c), (d) and (e)). Since the Al doping in the ZnO crystal structure could be neglected, the thin films had low carrier concentration.

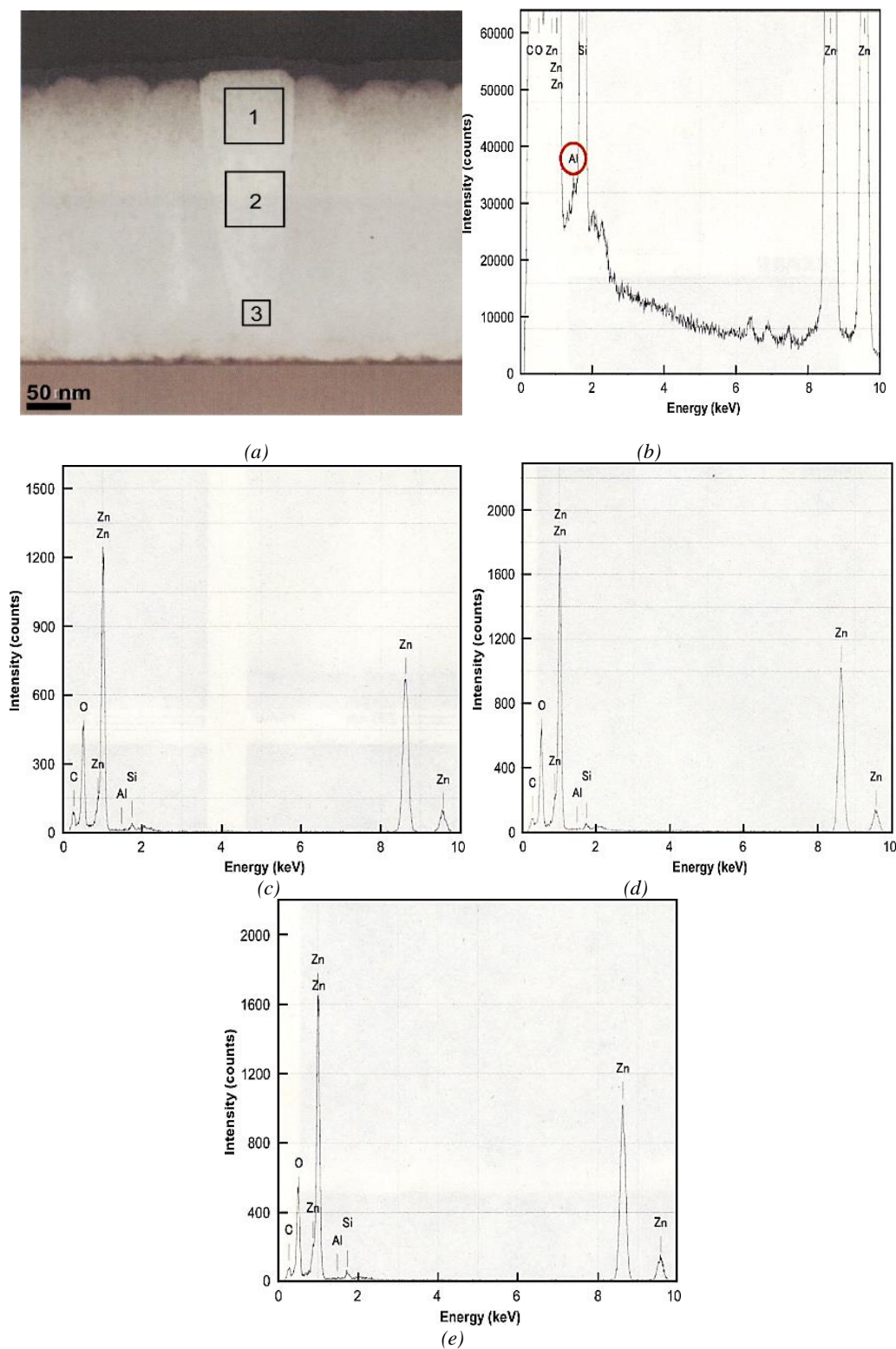


Fig. 6. (a) Cross-sectional high-angle annular dark field scanning transmission electron microscopy (HAADF STEM) image of AZO thin film deposited on Si substrate, (b) the energy-dispersive X-ray analysis (EDX) result of (a), and the EDX results of part 1 (c), 2 (d) and 3 (e)

4. Conclusions

The (002)-oriented AZO thin films with columnar cross-section were deposited on the fused quartz glass substrates with (002)-oriented ZnO nucleation layer by the chemical bath deposition. The carrier concentration ranged from 1.82×10^{19} to 4.40×10^{19} cm⁻³, while the carrier mobility changed between 4.40 cm²/(V·s) and 20.0 cm²/(V·s). The Al³⁺ ions mainly segregated at the grain boundaries in the thin films, and the Al doping in ZnO crystal structure was almost negligible, which induced the low carrier concentration.

Acknowledgements

This work was financially supported by 111 project of China (No. B13035) and the Fundamental Research Funds for the Central Universities (WUT: 2016III020).

References

- [1] B. H. Kim, C. M. Staller, S. H. Cho, S. Heo, J. Kim, D. Milliron, *ACS Nano* **12**, 3200 (2018).
- [2] B. B. Sahu, B. J. Su, P. J. Xiang, J. B. Kim, J. G. Han, *J. Appl. Phys.* **123**, 205107 (2018).
- [3] P. Mbule, D. Wang, R. Grieseler, P. Schaaf, B. Muhsin, H. Hoppe, B. Mothudi, M. Dhlamini, *Solar Energy* **172**, 219 (2018).
- [4] D. George, L. Li, D. Lowell, J. Ding, J. Cui, H. Zhang, U. Philipose, Y. Lin, *Appl. Phys. Lett.* **110**, 071110 (2017).
- [5] M. Birkholz, B. Selle, F. Fenske, W. Fuhs, *Phys. Rev. B* **68**, 205414 (2003).
- [6] R. Chandramohan, T. A. Vijayan, S. Arumugam, H. B. Ramalingam, V. Dhanasekaran, K. Sundaram, T. Mahalingam, *Mater. Sci. Eng. B* **176**, 152 (2011).
- [7] C. Verrier, E. Appert, O. Chaix-Pluchery, L. Rapenne, Q. Raffay, A. Kaminski-Cachopo, V. Consonni, *Inorg. Chem.* **56**, 13111 (2017).
- [8] M. Advand, M. Kolahtouz, A. Rostami, M. Masnadi-Shirazi, M. Norouzi, A. H. Karami, N. Hajiabdollahi, *Thin Solid Films* **656**, 6 (2018).
- [9] D. Guo, K. Sato, S. Hibino, T. Takeuchi, H. Bessho, K. Kato, *J. Mater. Sci.* **49**, 4722 (2014).
- [10] D. Guo, K. Sato, S. Hibino, T. Takeuchi, H. Bessho, K. Kato, *Thin Solid Films* **550**, 250 (2014).
- [11] D. Guo, Y. Ju, C. Fu, Z. Huang, L. Zhang, *Mater. Sci.-Poland* **34**, 555 (2016).
- [12] H. Tanaka, K. Ihara, T. Miyata, H. Sato, T. Minami, *J. Vac. Sci. Technol. A* **22**, 1757 (2004).
- [13] J. Hu, R. G. Gordon, *J. Appl. Phys.* **71**, 880 (1992).
- [14] N. Kumar, A. Dubey, B. Bahrami, S. Venkatesan, Q. Qiao, M. Kumar, *Appl. Surf. Sci.* **436**, 477 (2018).
- [15] B. Nasr, S. Dasgupta, D. Wang, N. Mechau, R. Kruk, H. Hahn, *J. Appl. Phys.* **108**, 103721 (2010).

*Corresponding author: guody@whut.edu.cn